Supporting Information for:

Toward the Meta-Atom Library: Experimental Validation of Machine Learning-Based Mie-Tronics

Hooman Barati Sedeh[1], Renee C. George[1], Fangxing Lai [2], Hao Li [2], Wenhao Li[1], Yuruo Zheng[1], Dmitrii Tstekov[1], Jiannan Gao[1], Austin Moore[3], Jesse Frantz[3], Jingbo Sun[4], Shumin Xiao[2], and Natalia M. Litchinitser[1, *]

[1]Department of Electrical and Computer Engineering, Duke University, Durham, NC, USA

[2]Ministry of Industry and Information Technology Key Lab of Micro-Nano Optoelectronic Information System, Harbin Institute of Technology Shenzhen, 518055 Shenzhen, P. R. China.

[3]Naval Research Laboratory, Washington, DC, USA

[4]School of Materials Science and Engineering, Tsinghua University, Beijing, 100084, China

*natalia.litchinitser@duke.edu

- This Supporting Information is organized into seven sections and intended to provide additional information about the implemented training dataset, the effects of various parameters on the scattering spectra, and more experimental details on the fabricated samples.

Supplementary Note 1: Geometry of the Implemented Dataset

The training and validation of ML models in this study relied on a dataset from our previous work [19], comprising two specific geometry sets called '*regular*' and '*irregular*' shapes. In particular, the regular set incorporates 1300 meta-atoms, each distinguished by its shape, characterized on the $(x-y)$ plane as

$$x = R[\cos(\varphi) + \alpha\cos(2\varphi) + \beta\cos(3\varphi)]$$
$$y = R[\sin(\varphi) + \gamma\sin(2\varphi) + \zeta\sin(3\varphi)] \quad \textbf{(S1)}$$

wherein $R = 160$ nm, φ denotes the azimuthal angle within the range of $[0, 2\pi]$ on the $(x-y)$ plane, and the dimensionless parameters α, β, γ, and ζ, varying between 0 and 0.6, are employed to modify the shape of the meta-atoms as was demonstrated in Figure 1 of the main manuscript. **Figure S1** (left side) shows a sample of six distinct

meta-atoms from the total collection of 1300 shapes as the representative example. To further enrich the variety of the geometries within our implemented dataset and increase the probability of exciting higher-order multipolar contributions within the meta-atoms, we have also included irregular shapes, as shown on the right side of Figure S1.

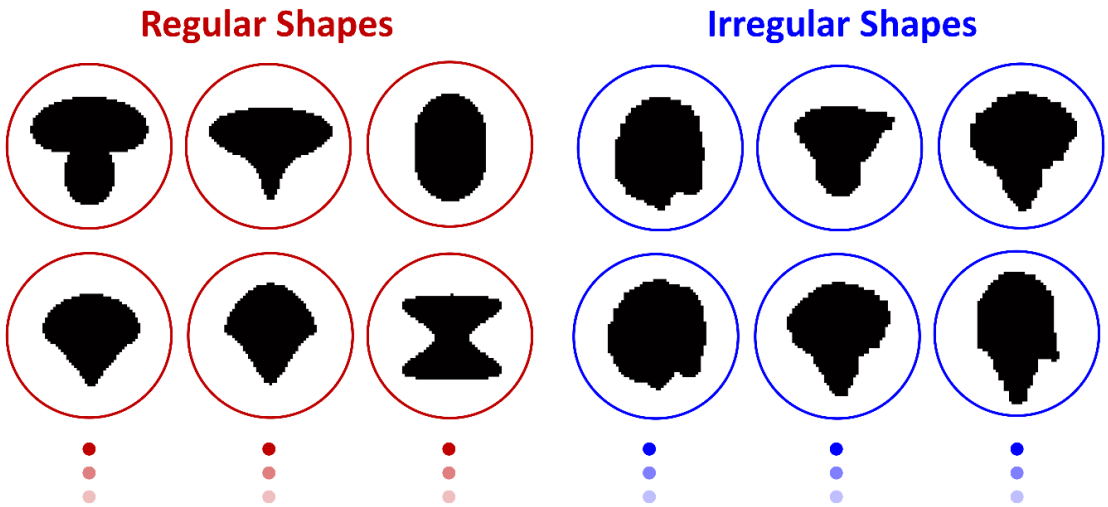

Figure S1. Implemented geometries within the dataset. Representative examples of both regular (left side with red color) and irregular (right side with blue color) geometries utilized to train the developed ML models. The regular topologies were defined mathematically, whereas the irregular forms were obtained through random perturbation of the regular shapes via a poorly trained inverse design model [19].

Supplementary Note 2: Ellipsometry Measurements of Glass and TiO_2

The previously developed IDM was trained based on the assumption that the refractive index of the meta-atoms follows the values reported by Sarkar et al. [33], as shown with dashed lines in **Figure S2(a)**. On the other hand, our ellipsometry measurements of the thin TiO_2 film have revealed a discrepancy of ≈5% in the values of refractive index, as shown in the same panel with a solid line. We have also measured the glass substrate's refractive index, as shown in Figure S2(b).

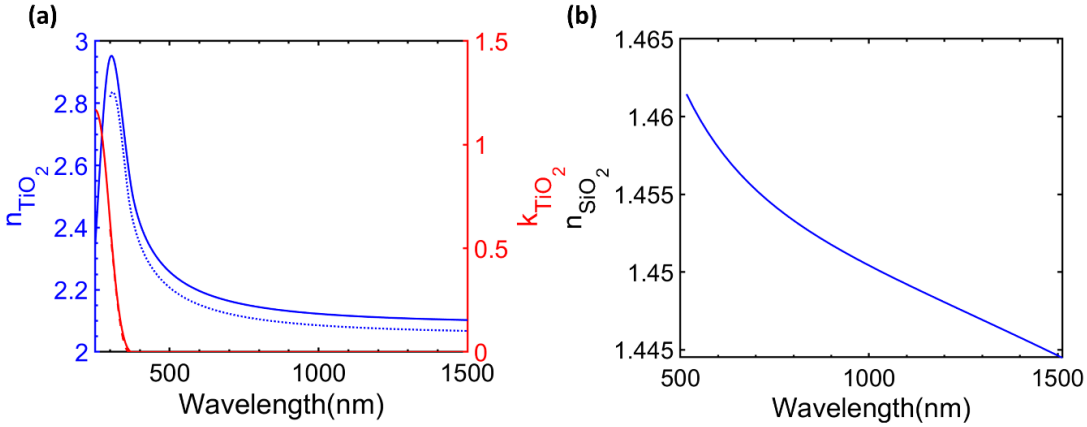

Figure S2. Measured refractive indices of the materials. The ellipsometry measurement of **(a)** TiO_2 wafer and **(b)** SiO_2 substrate. Blue represents the real part of the refractive index, while red represents the imaginary part. The dashed lines in panel (a) show the corresponding values reported by Sarkar et al. [33], and the solid line depicts the measured results of the fabricated sample.

Supplementary Note 3: Mie-Type Resonances in the Presence of a Substrate

The optical behavior of individual meta-atoms within homogenous host materials can be theoretically described using the multipole decomposition [44]. However, introducing substrates breaks down the separability of the Helmholtz equation, rendering the separation of variables method ineffective. Although image theory can be employed as the first-order approximation to tackle this problem, the applicability of this method is limited and complicated as it necessitates the replacement of point charge images with specific distributions [45]. We note that despite the recent proposal of a more comprehensive and rigorous approach to estimating the substrate effects, which involves shifting the coordinate origin from the scatterer's center to the substrate's surface, this method alters the definition of multipole moments from their conventional counterparts, leading to a misleading interpretation of optical responses [45-48]. In our study, we preferred to maintain the origin at the center of the meta-atom for consistency in the definition with most of the literature. In this perspective, one of the commonly used techniques for analyzing scattering phenomena in the presence of an inhomogeneity with a consistent definition is to examine the field distributions before and after the inclusion of substrate, as shown in Figure 2 of the main manuscript. While developing analytical methods for deriving multipoles centered on a scatterer placed on a substrate is undoubtedly intriguing, an approximate estimation of the contribution of the multipole moments is still required. To this aim, instead of assuming a refractive index mismatch between the superstrate and substrate, we set the refractive index of the surrounding environment to be the average value of the top and bottom media as $n_{\mathrm{bg}} = \left(n_{\mathrm{air}} + n_{\mathrm{SiO_2}}\right)/2 = 1.25$ and apply the conventional expression of the multipole moments for each predicted meta-atom [48], as shown in **Figure S3(a-c)**. By doing so, the contribution of the multipole moments in the presence of a substrate can be *approximately* evaluated, which, together with the field distributions, can serve as concrete evidence to gauge the validity of the ML-driven responses in realistic situations.

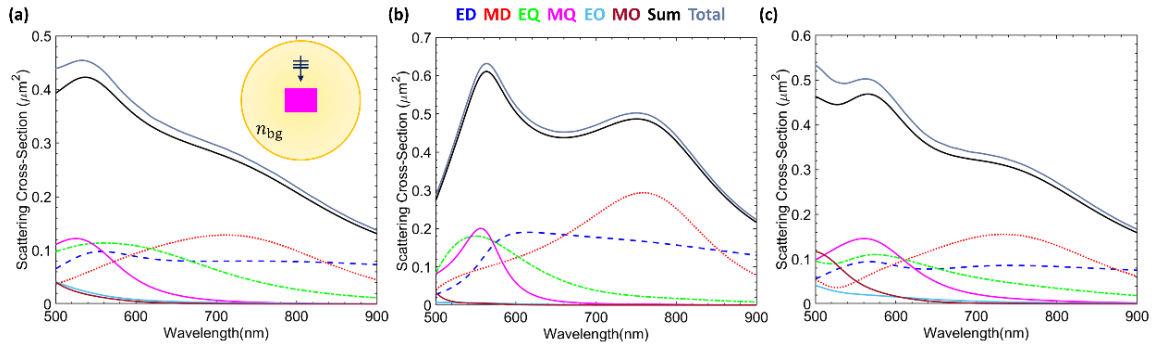

Figure S3. Approximate contribution of the multipoles in the presence of a substrate. The moments excited within the predicted meta-atoms supporting **(a)** ED, **(b)** MD, and **(c)** MQ Mie-like resonant modes in a homogenous medium with its refractive index being the average of superstrate ($n_{\mathrm{air}} = 1$) and substrate ($n_{\mathrm{air}} = 1.45$). The results obtained closely resemble the case of scatterers in an inhomogeneous medium.

It is evident that due to the decrement in the refractive index contrast between the meta-atoms and the surrounding medium from $\Delta n = 1.14$ to $\Delta n = 0.89$, the scattering response of the scatterers broadens, and their corresponding amplitudes decreases. However, despite these changes, the predicted response of the

meta-atoms' response in the modified homogeneous medium closely follows the air background case, suggesting that the substrate does not significantly alter the excited multipole moments inside the meta-atoms.

Supplementary Note 4: Role of Lattice Periodicity on the Multipoles Interactions

As mentioned in the main manuscripts, the lattice periodicity can significantly alter the optical response of the predicted meta-atoms. From this perspective, the lattice periodicity should be selected to minimize the coupling between the scatterers in the array and suppress their collective resonances. In the paper, we illustrated the results related to $p = 1\mu m$, and here we explore the role of other periodicities on the corresponding field distribution of the array at their specific designed wavelength. In particular, we numerically investigated five different lattice periodicities of $p = [0.6,0.8,1,2,3]\mu m$. We calculated the field distribution in the (x-y) plane as shown in **Figure S4 (a-c)** for meta-atoms supporting ED, MD, and MQ, respectively. For better visualization, we have intentionally saturated the color bar such that the intra couplings are better identified.

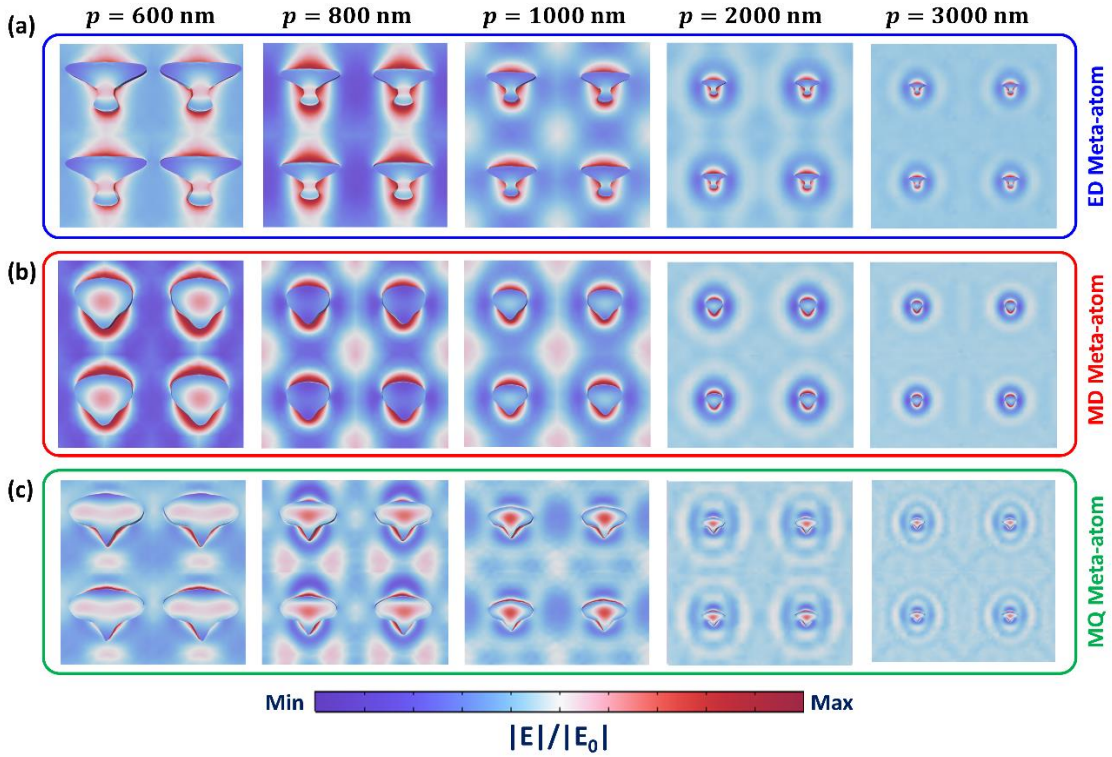

Figure S4. Lattice periodicity effect on the optical response of meta-atoms. The 3D distribution of the electric field within an array of meta-atoms corresponding to **(a)** ED, **(b)** MD, and **(c)** MQ Mie-type resonances with different lattice periodicities ranging from $p = 600$ nm to $p = 3000$ nm. As the periodicity increases, the effect of collective resonances and the coupling between scatterers decreases, yielding behavior similar to that of the isolated meta-atoms.

As can be seen from these figures, for subwavelength periodicities of $p = 0.6\ \mu m$ and $p = 0.8\ \mu m$, field distributions of the scatterers are significantly modified compared to their isolated counterpart, which is attributed to the coupling between the meta-atoms within the array. On the other hand, for periodicities larger than $p > 1\mu m$, the spatial field distribution of the array closely resembles its isolated counterpart, suggesting that the coupling between the meta-atoms has been effectively suppressed.

Supplementary Note 5: Angular Dispersion of the Predicted Meta-Atoms

It has been previously shown that the optical response of a subwavelength particle strongly depends on its orientation with respect to the direction of illumination such that certain spectral features emerge or get suppressed [28]. Such an angular dispersion stems from the changes in the components of multipolar moments within the meta-atom and the variations in the coupling efficiency of a particular Mie resonant mode as a function of illumination direction. Therefore, while tuning the illumination angle has been one of the key ingredients in controlling the optical response of meta-scatterers in recent years, it might be problematic for our case as the ML model was trained under the assumption of normal incidence. In this perspective, to gauge the effect of illumination angle on the optical response of the scatterers, we have theoretically studied the scattering cross-section of the meta-atoms on a glass substrate as a function of incident angle ($0^\circ < \theta_i < 45^\circ$) and operating wavelength as it is shown in **Figure S5(a-d)**.

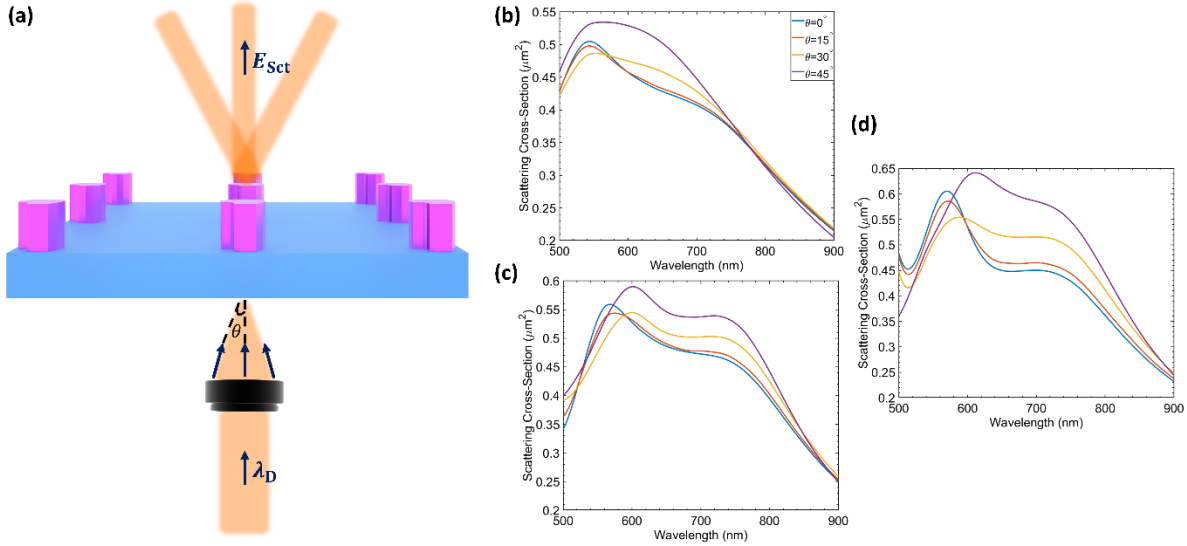

Figure S5. The role of illumination angle on the predicted optical response. (a) Artistic demonstration of meta-atom arrays under oblique illumination. The calculated scattering cross-section of the predicted meta-scatterers as a function of illumination angles for inverse designed **(b)** ED, **(c)** MD, and **(d)** MQ supporting meta-atoms. For incident angles of $\theta_i < 15^\circ$, the optical response of the subwavelength particles closely follows their normal incidence counterparts.

As can be seen from Figure S5(c-d), for illumination angles smaller than $\theta_i < 15^\circ$, the optical response of the meta-scatterers closely follows the normal incidence. In contrast, for $\theta_i > 30^\circ$, the scattering cross-sections are significantly altered due to the change in the contributing multipolar moments. Therefore, in the experiment, we lightly focused the incoming beam on the meta-atoms ($|\theta_i| < 15^\circ$) to avoid the effect of illumination directions on the optical response of the predicted meta-scatterers.

Supplementary Note 6: Role of Higher Diffracted Orders on the Optical Response

The interference of scattering fields gives rise to discrete diffraction orders, with their angles following $\sin(\theta_{mn}) = \lambda_D \sqrt{(m/p_x)^2 + \left(n/p_y\right)^2}$, wherein m and n indicates the diffracted modes, λ_D is the designed wavelength and p_x and p_y representing periodicity along x and y directions as it is schematically shown in **Figure S6(a)**. Although we have shown that for lattice periodicities above $p > 1\mu m$, the coupling between the scatterers is minimal, we have yet to discuss the efficiency of the generated diffracted orders and their

roles in the overall transmittance response. In this perspective, for the designed wavelength of $\lambda_{\mathrm{ED}} = 900$ nm, $\lambda_{\mathrm{MD}} = 780$ nm, and $\lambda_{\mathrm{MQ}} = 570$ nm, the possible diffraction angles (modes) can be shown to reach extreme values as it is illustrated in Figure S6(b-d) for lattice periodicities of $p = 1\mu m$, $p = 2\mu m$, and $p = 3\mu m$, respectively. In particular, regardless of the meta-atoms shape, the number of diffracted modes increases when the lattice periodicities tend to have larger values. Moreover, for the meta-atom supporting ED resonant mode, the total number of supported spatial frequencies is smaller than the rest of the scatterers, which is attributed to the fact that its ratio of λ_D/p is larger than its other two counterparts.

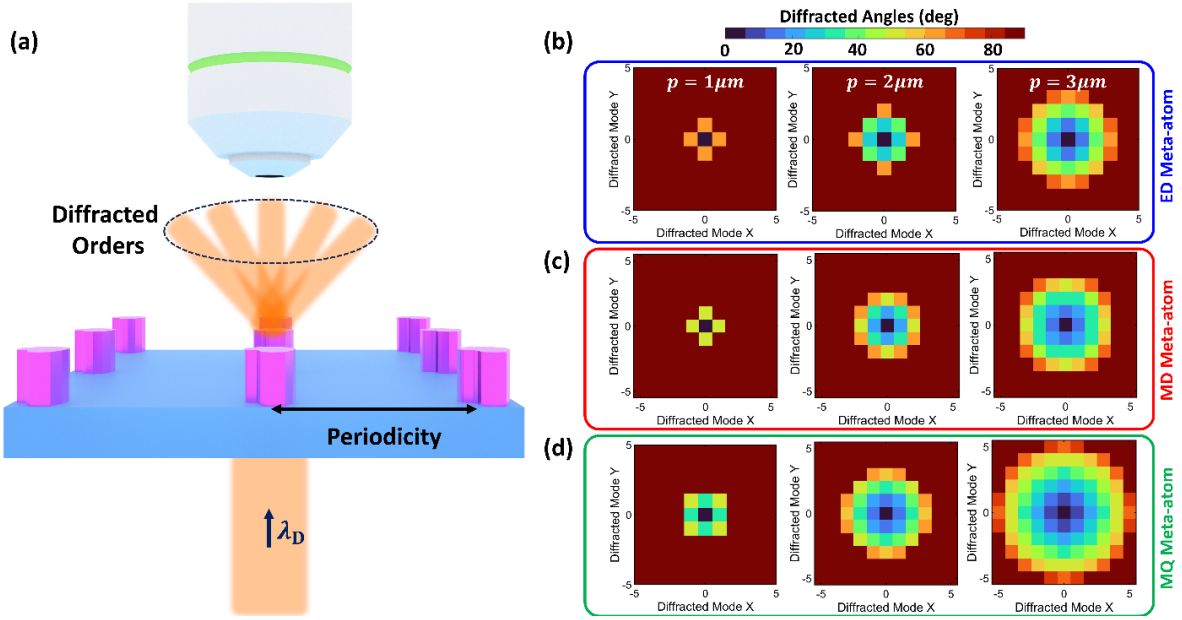

Figure S6. Possible diffracted orders of the meta-atom arrays. (a) Schematic illustration of the diffraction pattern of the meta-atom arrays. Once the periodicity becomes larger, the number of diffracted modes increases. The calculated possible diffracted modes of meta-atoms supporting **(b)** ED, **(c)** MD, and **(d)** MQ Mie-type resonances as a function of lattice periodicity. For scatterers whose ratio of λ_D/p is smaller, the number of possible diffracted modes is larger.

To gauge the energy that leaks to each of these generated diffracted modes, we have calculated their corresponding transmittance efficiency, $\%\eta_{mn} = (T_{mn}/\Sigma_i T_i) \times 100\%$, at their designed wavelength, as shown in **Figure S7(a-c)** for meta-atoms supporting ED, MD, and MQ, respectively. As can be seen from this figure, despite the existence of higher diffracted modes, the main scattering features are directly attributed to the fundamental (0,0) mode, with its lowest and highest efficiency reaching $\approx 61\%$ for the MQ scatterer and $\approx 99\%$ for the meta-atom supporting ED. Because of such a high contribution of the fundamental mode, it is safe to assume that higher diffraction orders play a negligible role in the optical response and attribute the total scattering to the (0,0) mode propagating along the incident direction.

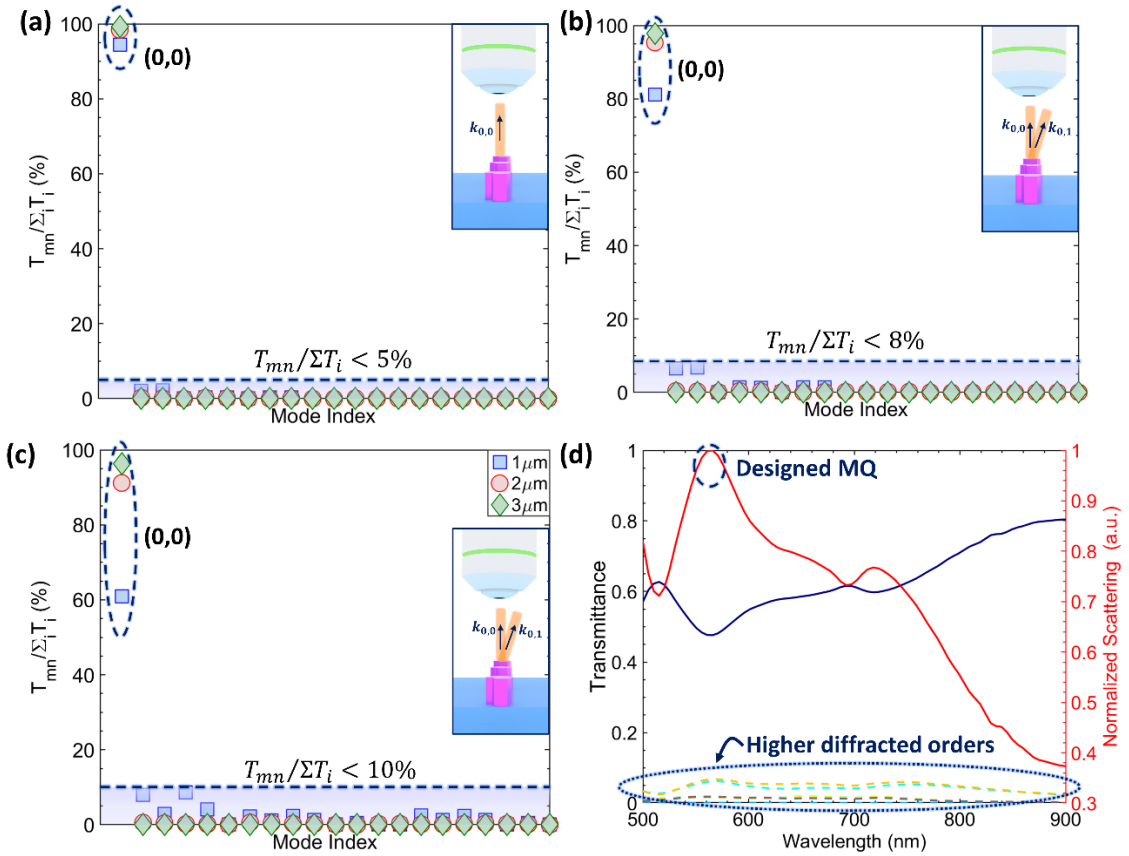

Figure S7. Optical response of the generated higher-order diffraction modes. The calculated meta-atom array transmittance efficiency at the designed operating wavelengths of **(a)** $\lambda_{\mathrm{ED}} = 900$ nm, **(b)** $\lambda_{\mathrm{MD}} = 780$ nm, and **(c)** $\lambda_{\mathrm{MQ}} = 565$ nm. The main contribution of the optical response for all the meta-atoms is attributed to $k_{0,0}$, while there is a negligible contribution of other modes. **(d)** The transmittance response of the MQ scatterer as a function of wavelength with a solid line denoting the (0,0) mode and a dashed line illustrating the higher diffracted orders. The scattering cross-section is also derived based on the calculated $T_{0,0}(\lambda)$ with red color.

Due to the diffractive nature of periodic structures, the diffracted modes can be more prominent at wavelengths other than the designed one, which might affect the overall scattering spectra compared to the isolated case. While the experimental measurements of the meta-atom arrays demonstrated a close resemblance to the isolated cases, which suggests that even for other operating wavelengths, the role of higher diffraction is negligible, we have also calculated the efficiency of the higher modes for the scatterer supporting MQ shown in Figure S7(d) to verify our measured results numerically. It should be noted that we merely studied this case as its scattering efficiency for $p = 1\mu m$ showed the minimal value compared to the ED and MD meta-atoms, shown in panel (c), suggesting that the role of higher diffracted modes might be more prominent. However, as can be seen from the calculated response, the diffraction pattern indicates that the main feature of the optical response is directly attributed to the fundamental mode (solid navy color line) even at other operating wavelengths, with a negligible contribution of higher diffraction modes (dashed color lines). We have also calculated the scattering cross-section, illustrated in red, from the fundamental mode, showing good agreement with the experimental results. As the final remark, we note that while in the experimental setups, higher numerical aperture (NA) objectives can be used in the collection arm to capture all the generated diffracted modes, our theoretical investigations indicate that due

to the negligible contribution of these generated modes, one can use even lower NA objectives than what we used in our setup ($\mathrm{NA} = 0.25$) and still collect the scattering response of the designed meta-atoms.

Supplementary Note 7: Effects of Inclined Sidewalls and Refractive Index Difference

As was mentioned earlier, our previously developed IDM was trained based on the assumption that the refractive index of the training meta-atoms follows the values reported by Sarkar et al. [33]. However, our ellipsometry measurements of the fabricated thin film revealed a discrepancy of $\approx 5\%$ in the values of the refractive indices, as shown in Figure S2(a). Such a difference in the refractive indices leads to a spectral shift within the predicted scattering spectra, as shown in **Figure S8(a-c)**.

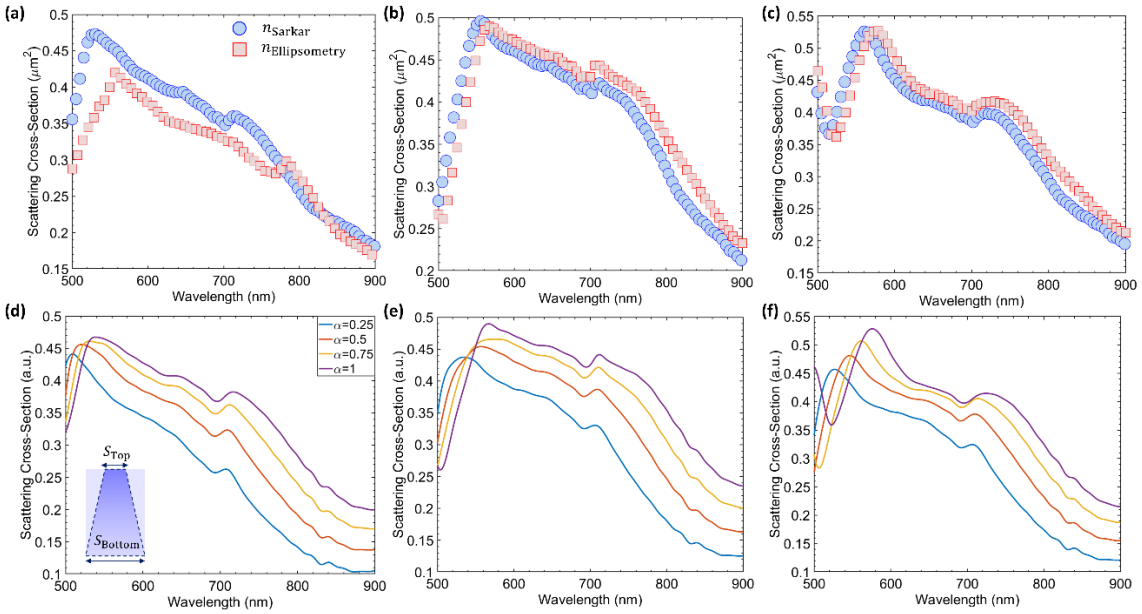

Figure S8. Effects of Inclined Sidewalls and Refractive Index Difference. Calculated total scattering cross-sections of the meta-atoms supporting **(a)** ED, **(b)** MD, and **(c)** MQ resonant modes when the refractive index follows reported values by Sarkar et al. (blue circle) and the ellipsometry measurements (red squares). **(d-f)** Total scattering cross-sections of the predicted meta-scatterers when the side walls alter from perfectly vertical ($\alpha = 1$) to inclined ($\alpha \neq 1$).

In addition, due to the $\mathrm{TiO_2}$ etching process and the Cr removal phase, the side walls of the fabricated meta-atoms are not perfectly vertical. To approximately gauge the effect of these discrepancies on the optical response of the predicted meta-atoms, we have defined the ratio of $\alpha = S_{\mathrm{Top}}/S_{\mathrm{Bottom}}$, with S_i denoting the surface area of the top/bottom boundary of the meta-atom, and calculate the scattering cross-section of the scatterers for four representative cases of $\alpha = [0.25, 0.5, 0.75, 1]$ as shown in Figure S8(d-f). As can be seen from these figures, the transition of the sidewalls from vertical ($\alpha = 1$) to inclined ($\alpha \neq 1$) leads to spectral shift within the scattering spectra.